Design and evaluation of a modular instrument for endoscopic thyroid surgery

Master Thesis

Nienke van der Wal

To obtain the degree of Master of Science
at the Delft University of Technology
to be defended publicly on 30-05-2024

Student number: 4457684
Supervisor: Dr. Ir. Ing. T. Horeman
Thesis committee: Dr. Ir. Ing. T. Horeman
Prof. Dr. J. Dankelman
Christian Camenzulig (surgeon)

Department of BioMedical Engineering
Delft University of Technology

Abstract

Introduction The global incidence of thyroid cancer has risen significantly, prompting the development of innovative surgical techniques. Transoral thyroidectomy offers a scarless alternative, with the transoral endoscopic thyroidectomy vestibular approach (TOETVA) showing promising results. However, CO_2 insufflation during TOETVA can lead to fatal complications. To address these issues, researchers have explored gasless TOETVA methods. Our study introduces a modular articulating retractor integrated with a 5mm camera system, aimed at minimizing CO_2-related complications while preserving the benefits of the conventional procedure.

Method Through a design process comprising problem definition, ideation, and solution creation. A detailed digital CAD design is developed based on force measurements obtained from a preliminary cadaver study. Subsequently, a functional prototype is created and subjected to pre-clinical testing using Thiel-embalmed and fresh frozen cadavers.

Results Force tests determined a mean force of 4.73N across cadavers, with 5.29N necessary for optimal skin elevation. SolidWorks simulation indicated maximum stresses of 128.10 MPa and 113.80 MPa in articulated and horizontal positions. Backdrivability of articulation occurred at approximately 4N applied force. Assembly and disassembly tasks demonstrated mostly normal distribution, with significant differences observed between initial and final assembly attempts. Despite successful procedure performance, challenges included endoscope removal limitations and partial functionality constraints during articulation within cadavers. Overall removal time averaged 3.2s, with a maximum of 4.1s.

Conclusion The gasless TOETVA procedure was performed successfully with sufficient visualization for the surgeon. While achieving three of our four objectives, including the design and compatibility with standard endoscopic cameras, limitations prevented direct comparison with conventional CO_2-based TOETVA methods. Despite this setback, the initial incorporation of our instrument into surgical procedures demonstrates promise. However, further research is imperative to compare its performance against conventional methods, validating its efficacy and potential in clinical practice.

CONTENTS

1. INTRODUCTION

1.1. Background

The incidence of thyroid cancer has exhibited a significant increase over recent decades in numerous countries [1]. In the United States alone, an estimated 43,720 new cases of thyroid cancer were reported in 2023 [2]. This represents twice the number of cases compared to 30 years ago. Thyroid surgery plays an important role in the management of these occurrences, with four distinct types: total lobectomy or hemithyroidectomy (TL), subtotal thyroidectomy (ST), total thyroidectomy (TT), and substernal thyroidectomy (SST). In a lobectomy, one half of the thyroid gland is removed while the other remains intact. Subtotal thyroidectomy entails the removal of most of the thyroid gland, sparing specific tissue on the bilateral posterior aspect to minimize the risk of recurrent laryngeal nerve (RLN) damage. A total thyroidectomy involves the complete removal of the thyroid gland.

The golden standard procedure for thyroid surgery is open surgery [3]. In this procedure, an incision known as the "Kocher incision," measuring 3 to 7 cm, is made in the anterior neck through which the surgery is performed. However, a concern with this surgery is the visible scar on the neck, which can have a negative impact on the quality of life [4].

Through the development of endoscopic thyroidectomy, surgeons are able to minimize or eliminate the visibility of the scar. Various extra-cervical endoscopic thyroidectomy include the transaxillary approach [5][6][7], anterior thoracic approach [8], breast/chest approach [9], hybrid approaches, postauricular facelift approach [10], and transoral approach. The transaxillary approach involves accessing the thyroid through three axillary incisions, demonstrating positive outcomes in cosmetic results and postoperative pain reduction [7]. However, the longer distance to the thyroid requires extensive dissection, posing challenges in accessing the contralateral thyroid lobe and RLN from a single side [11]. In the breast approach, two ports are inserted into the breast, and one is inserted into the parasternal area [9]. The wide breast angle provides a broad field of vision, enhances instrument maneuverability, and limits collision between the instruments. In the anterior thoracic approach, a 3 cm incision is made in the chest, just below the clavicle. This displaces the scar lower on the chest for better concealment with clothes [8]. In the postauricular facelift approach, the incision is made below the ear along the hairline. The benefits of the postauricular facelift are that it has a relatively smaller dissection area and a shorter distance from the incision site to the thyroid gland than the other approaches. However, the working space is narrow, and approaching and removing the contralateral thyroid lobe is difficult [10]. All approaches are shown in Figure 1.

While the transaxillary, anterior thoracic, breast/chest, and postauricular approaches redirect scars to concealed areas when clothed, they are not entirely scarless. Moreover, these approaches often necessitate extensive dissection to reach the targeted site, and some approaches may exhibit limitations such as small working space and restricted two-dimensional vision [3]. In response to these challenges, transoral thyroidectomy emerged as an alternative. This approach has no visible scar since all incisions are made within the oral cavity. The first endoscopic attempts were conducted on animals and cadavers [12]. This led to the introduction of endoscopic minimally invasive thyroidectomy (eMIT) on humans, performed by Wilhelm *et al.* [13]. This method involved piercing the floor of the mouth, combined with two vestibular incisions utilizing Kirshner wires for skin elevation in a gasless technique. Despite offering limited laparoscopic vision, restricted movement, and challenges in converting to open surgery, it paved the way for further advancements. Wang *et al.* [14] performed endoscopic thyroidectomy oral vestibular approach (ETOVA) using CO_2insufflation in 24 patients. This effort evolved into the transoral endoscopic thyroidectomy vestibular approach (TOETVA) [15]. TOETVA improved the floor-of-mouth technique due to the shorter recovery times, lower operative time, and reduced postoperative infections [15]. A comparative study involving 425 patients treated with TOETVA and open thyroidectomy (OT) was conducted by Anuwong *et al.* [16]. Results indicated a significantly longer operative time for TOETVA compared to OT. However, no significant differences were observed in estimated blood loss or complication rates, thus deemed safe to use.

During TOETVA, the working space of the surgical site is developed and maintained using CO_2. Although the procedure proves to be safe and effective compared to OT, there are some complications that the CO_2 insufflation may lead to. Some of the known complications include subcutaneous emphysema, pneumothorax, pneumomediastinum, and CO_2 embolism [17][18]. Although a CO_2 embolism does not occur often, it can be fatal. It is caused by the entrapment of carbon dioxide in an injured vein or artery, blocking the right ventricle or pulmonary artery [19].

To overcome these problems, researchers have explored the implementation of a gasless TOETVA. Among the various attempts, a commonly employed method involves a space suspension system inserted through the central vestibule incision, which is affixed to the anesthesia stand [20][21][22]. However, a drawback of this approach is the possible interference caused by the stand to which it is attached. An alternative approach involves redesigning the trocar to incorporate a fan retractor, thereby creating space [23]. Nevertheless, this design presents challenges in converting to open surgery in cases of bleeding. Another preclinical design proposed by Camenzuli *et al.* [24]

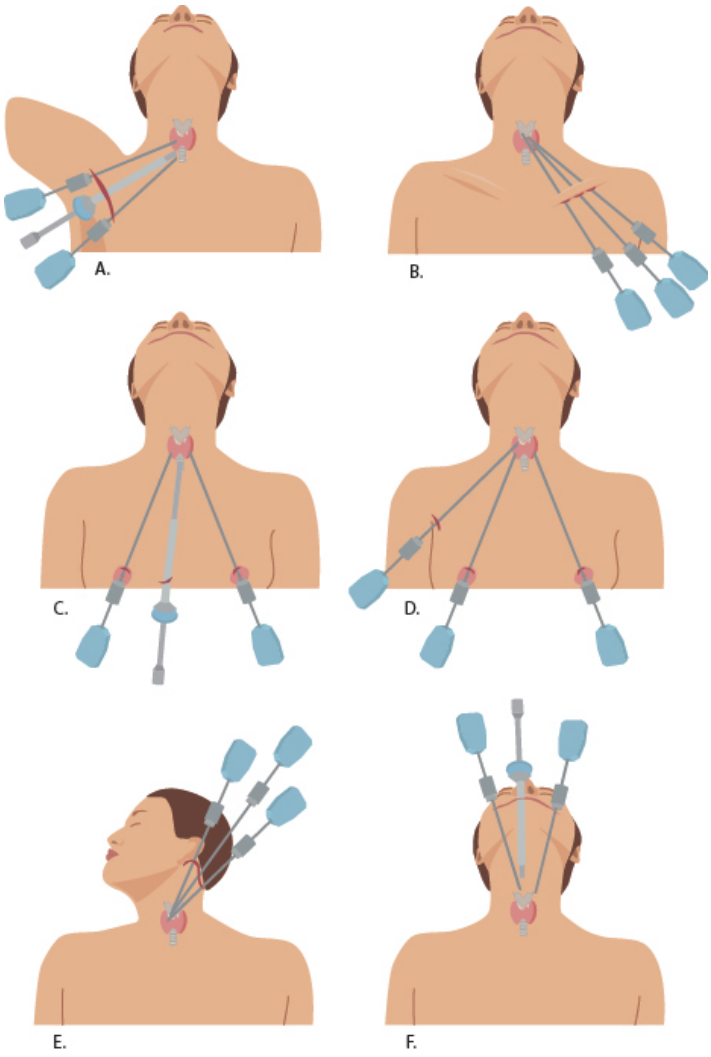

Figure 1: A. Trans-axillary approach; B. Clavicle approach; C. Breast/chest approach; D. Hybrid approach (e.g. bilateral axillo-breast approach); E. Postauricular facelift approach; F. Trans-oral approach

introduces a tool that fits through a trocar. This device integrates the endoscope into the fan retractor, fitting through the 10mm trocar. However, during testing, the fan was obstructing the vision of the endoscope.

In this study, we developed an articulating retractor to create a surgical space integrated with the standard TOETVA method to avoid CO_2-related problems. The main advantage of the device is that it creates more workspace while also allowing a 5mm endoscope to fit through the device, mitigating the need for a fourth port.

1.2. Anatomy thyroid

The thyroid gland is an endocrine organ in the neck, anterior to the trachea and inferior to the larynx. It has a butterfly shape and consists of two lobes (left and right) that connect to the isthmus at the center [25]. These lobes wrap around the cranial portion of the trachea. Posterior to the lobes are four parathyroid glands—two superior and two inferior—that produce parathyroid hormone and are typically preserved during a thyroidectomy. However, their exact location can vary among individuals, making localization and preservation challenging. Superficial to the thyroid are the strap muscles, including the sternothyroid, thyrohyoid, and sternohyoid muscles. The platysma is a thin muscular layer separating the strap muscles from the skin. The thyroid gland is highly vascularized, receiving a substantial blood supply from the superior thyroid artery and the first branch of the external carotid artery. Venous drainage occurs via the superior thyroid vein, close to the superior thyroid artery, inferior thyroid vein, and middle thyroid vein. The recurrent laryngeal nerve (RLN) runs posterior to the thyroid, adjacent to the trachea. This nerve is crucial for controlling the muscles of the vocal cords, emphasizing the importance of avoiding damage during the procedure. For an overview of the simplified anatomy, see Figure 2. For a complete frontal anatomical overview, see section A.

1.3. Operative steps of TOETVA using CO_2

The methodology outlined by Diogini *et al.* [26] is organized into five sections for ease of referencing throughout this paper. The particular emphasis within this research is placed on the sections related to 'incision and insertion' and 'space building and maintaining' because the device's application occurs in these specific sections when replacing CO_2 insufflation with a mechanical space-making system. The remainder of the surgical process remains consistent with the procedure using CO_2 insufflation.

- **Positioning:** The patient is put under general anesthesia and placed in a supine position with the neck slightly extended, supported by a shoulder block. The bed is at a 15-textdegree angle in the Trendelenburg bed position.
- **Incisions and insertion:** An endotracheal tube is inserted and secured at one corner of the mouth. The oral cavity is disinfected with antiseptic, followed by a 10-15mm incision in the central oral vestibular area of the lower lip along the midline. Blunt dissection in the subplatysmal layer creates a space through which the 10mm blunt-tipped central port is inserted. At this time, the CO_2 insufflation is introduced. The space is developed using CO_2 insufflation pressure of 6-8 mmHg. Two additional 5mm incisions are made below the canine teeth on both sides while carefully

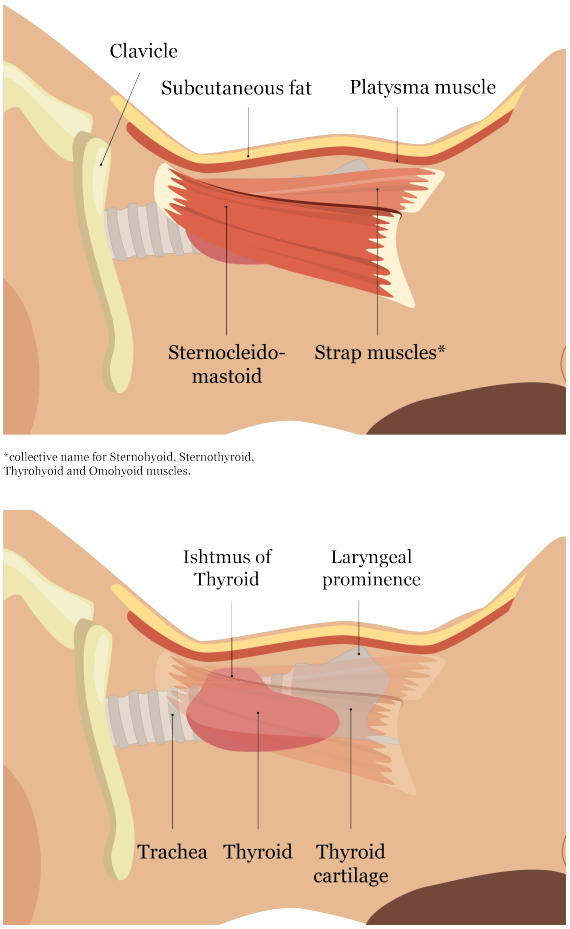

Figure 2: Simplified anatomy of the neck region in a side view

avoiding damage to the mental nerve, which provides sensation to the jaw, chin, and lower lip. Two additional ports are inserted to introduce the forceps.

- **Space developing and maintaining:** Passing the mandibular area and submental plane, a space is developed beneath the skin, subcutaneous fat, and the platysma muscles, and above the strap muscles, creating the surgical workspace as seen in Figure 5. This development is done using both sharp and blunt dissection. The strap muscles are divided and retracted by cutting midline linea alba cervicalis and deep fascia. Strap muscles are retracted to the ipsilateral side using a hook to expose the thyroid isthmus.
- **Retrieval of gland:** Once the thyroid is identified, the isthmus is dissected off the underlying trachea, lifted off the trachea, and centrally cut to better access the posterior side of the thyroid, where the laryngeal nerves and parathyroid glands are located. The superior artery and vein are identified and dissected, followed by detection and transection of the inferior thyroid artery. After clearing the vessels, the thyroid lobe is dissected along the tracheal wall to the inner edge of Berry's ligament, ensuring careful division of Berry's ligament to avoid damage to the recurrent nerve and parathyroid glands. The same dissection process is repeated on the other side, and upon freeing both of the lobes, the specimen is removed using an endo bag through the central port.
- **Closure:** The pretracheal fascia surrounding the strap muscles is sutured together to prevent the trachea from adhering to the neck skin. The operative area is rinsed with a saline solution, and the vestibular surgical wounds are closed using absorbable sutures.

1.4. Aim and Objectives

To minimize the CO_2 related problems associated with thyroid surgery (and to increase the maneuverability), an instrument needs to be developed and tested that can be used manually by a surgeon. It can easily maneuver to the operating site and maintain the space in this area without using gas. With this in mind, the following goal is determined.

> *The aim is to design an instrument that provides surgeons with clear visualization and a spacious workspace during gasless trans-oral video-assisted thyroidectomy (TOETVA) while preserving the benefits of the conventional method that utilizes CO_2 insufflation.*

This leads to the following objectives:

- Design a gasless guidance trocar with space-maintaining capabilities suitable for use with a standard endoscopic camera.
- Create a fully functional blueprint model production and characterization that meets all requirements.
- Evaluate and compare the performance of the new trocar design against conventional TOETVA methods employing gas insufflation in a preclinical setting.
- Enhance surgical procedures by incorporating the newly designed functional instrument into the workflow.

2. Method & Materials

2.1. Technical requirements

The device has been designed to comply with requirements set based on literature and conversations with an expert in the field of TOETVA. The requirements are stated below.

1) The device should maintain a workspace for the surgeon to have a clear visualization of the thyroid anatomy, which translates to a maximum width of 50 mm and a minimum length of 50 mm of the tip in the expanded state of the device.
2) The device should create a space above the thyroid with a minimum height of 30 mm to allow for adequate freedom of movement for the endoscopic tools. This is to accommodate the (steerable) tips, which have a length of approximately 30 mm when pointed downwards.
3) The outer diameter of the device in its smallest state should be no more than 10 mm. This is to accommodate insertion through a 10mm trocar cannula which is used in a standard TOETVA procedure.
4) The device must have a space for a standard 5mm endoscope to be inserted and used during the surgery.
5) The insertable part of the device must have a minimal length of 150mm to be able to reach the surgical site and to accommodate the 100mm length of the trocar.
6) The tip of the instrument should be able to articulate with a force of 10N without undergoing deformation. This is double the force needed to lift the skin in the neck.
7) All regions of the device must be able to be reached by the appropriate standard cleaning brushes for cleaning, which in the case of closed regions means the device must be modular and able to be disassembled to be able to reach these areas [27].
8) The instrument must be able to be sterilized using common sterilization methods (autoclave).
9) The device should not obstruct the endoscope's field of view when the retractor is fully articulated.
10) It should be possible to execute the procedure with two endoscopic instruments without collision with the camera system.
11) The device can be assembled by a single person in less than 110 seconds [27].
12) The device can be disassembled by a single person in less than 110 seconds [27].
13) In case of bleeding, the device should be removable within 3 steps and within 12 seconds to free up the neck area for traditional open thyroid surgery.

2.2. Performance criteria

The performance criteria are derived from the technical requirements. They are used in a Harris profile to evaluate the design concepts and make a weighted decision about which concept to continue with. The performance criteria are listed below.

- Ease of use
- Weight
- Durability
- Working volume
  - Size
  - Shape
- Setup time

2.3. Design process

The complete design process consists of multiple phases, including problem defining (and sub-problems), ideating solutions, creating solutions, and prototyping and testing. Once the requirements and criteria are established, the sub-functions of the device are outlined. Subsequently, these sub-functions form one axis of the morphological chart. For each sub-function, a mindmap is made using brainstorming sessions and literature searches. The sub-problems serve as focal points in the mind maps, with the solutions comprising the other axis in the morphological chart [28]. Upon completion of partial ideation and exploration of sufficient ideas, they are integrated into the final morphological chart. Selecting one solution from each sub-function generates 'principle solutions'. This process is repeated three times to provide three principle solutions, also called concepts. When three viable solutions are identified, they undergo evaluation using a Harris Profile in consultation with a surgical expert specializing in thyroid and TOETVA surgery. The most promising concept is then developed into a detailed digital (CAD) model and refined iteratively until it evolves into a functional working prototype. Subsequent iterations involve brainstorming sessions with assembly and manufacturing experts to refine the concept into a manufacturable design. Design choices consider factors such as costs, machine availability, assembly, time, capability, and capacity. Finally, a working prototype is constructed to test in a pre-clinical setting. The physical manufacturing of the device is executed in collaboration with Dienst Elektronische en Mechanische Ontwikkelingen (DEMO) at the TU Delft. More detail on the entire design process is provided in section B.

2.4. Study design

This research aimed to design an instrument that provides a spacious workspace during TOETVA while preserving the benefits of the conventional method using CO_2 insufflation.

2.4.1. Functional requirements

The maximum retraction width and articulation angle are measured. Since the articulation angle affects the maximum retraction width, the maximum retraction is measured when the tip is at its maximum articulation. A preliminary test is performed to determine the appropriate force required to displace

Figure 3: Test setup in the pre-clinical cadaver study. The force is measured using a spring scale attached to a rod, which in turn is affixed to the layers of the skin with suture thread. The width of these sutures is 40mm to simulate the width of the fans when in the maximum retracted position.

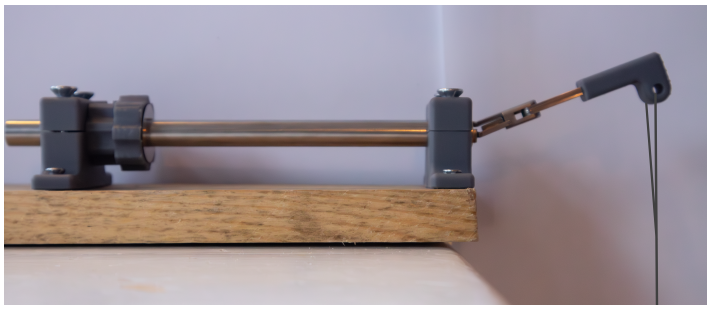

Figure 4: Test setup for the force test. The prototype is secured in a holder, and a weight of 5N is placed at the end of the fans.

the neck tissue for requirement 6. The force is quantified using a spring scale, with two threads inserted through the tissue layers requiring elevation, positioned 40mm apart to mimic the fan width. These threads are then connected to the spring scale, which is subsequently pulled upwards until the surgeon determines that an adequate workspace has been attained. The force required to reach this distance is measured. The setup is shown in Figure 3. This force is used as an input in a SolidWorks simulation to evaluate the stress levels. The force is applied vertically to the tips of the fans in both articulated and horizontal positions to simulate the most extreme scenarios. The simulation is run for situations in which the hinges connected to the control rod and holder rod are fixed, as well as when the fan holder is fixed.

Subsequently, this force is applied to the prototype to assess whether the articulation and retraction mechanisms can withstand it. In this test, a weight of 5N is attached to the tip and articulated 10 times. The device is secured by two holders attached to a table, maintaining it straight during articulation. The articulation angle is measured, and the tip is inspected for damage after each articulation cycle. The experimental setup for the force measurements is detailed in Figure 4.

2.4.2. User requirements

Its ease of assembly and disassembly is tested to assess the device's suitability for the Central Sterile Services Department (CSSD). This evaluation aims to determine whether assembly and disassembly can be accomplished within a reasonable time frame and without causing damage to the parts. In this experimental procedure, ten students were tasked with assembling and disassembling the device six times. Before the experiment, the students received step-by-step instructions from an instructor and had the opportunity to practice twice, receiving feedback from the instructor. Following their practice sessions, they were required to complete the assembly and disassembly tasks six times while timed. None of the students had prior experience with this instrument outside the training environment.

2.4.3. Pre-clinical test

To test the functional requirements in a clinical setting, a thyroidectomy procedure was performed on two Thiel-embalmed cadavers and two fresh frozen cadavers recruited from the University of Malta. The subjects were selected based on virgin neck anatomy, ensuring integrity from the chest upward to provide an optimal anatomical model. The procedure followed the steps outlined by [26]. However, CO_2 insufflation was not utilized; instead, blunt and sharp dissection techniques were employed to develop the subplatysmal space until there was enough space for the device to be introduced. A standard 5mm endoscope is fixed to the retractor device by use of the bolt, and the device is inserted through the trocar with the fins in a collapsed position and not articulated. When the device was completely developed, the assistant was asked to turn the knob for the fans in a clockwise motion to retract the fans in an outward motion. Then the assistant was asked to turn the knob for the articulation in an anticlockwise motion to articulate the tip upwards. Space maintenance relied on the retractor device rather than CO_2 insufflation, as depicted in Figure 5. The time taken for removal of the device from the cadavers was recorded.

2.5. Data analysis and interpretation

Statistical analysis was performed in IBM SPSS statistics (version 29.0.2.0 (20)). For the assembly and disassembly test, a Shapiro-Wilk test was conducted to indicate the normal

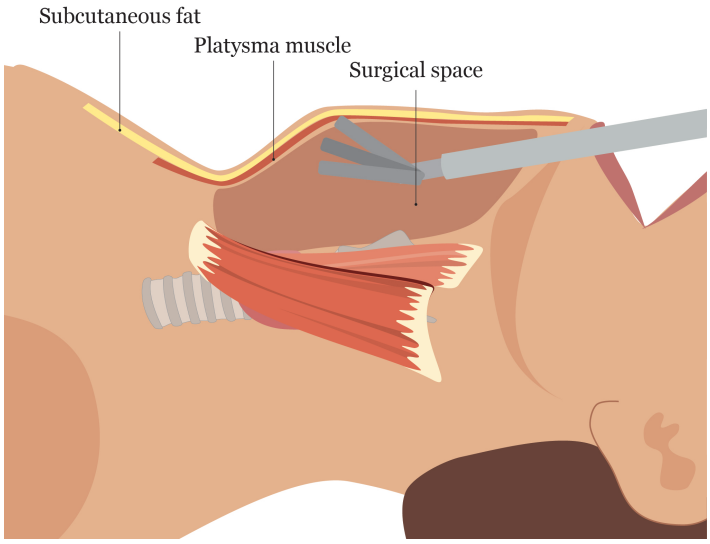

Figure 5: Surgical space

distribution of the data ($p > 0.05$). The trials were analyzed separately for normality; a paired t-test was used for a normal distribution. In the case of non-normally distributed data, the Wilcox Rank test was used. The first and last trials of the individual datasets were compared to determine if there was a learning effect. Differences were determined significant for $p < 0.05$.

2.6. Materials

Two Thiel-embalmed cadavers and two fresh frozen cadavers have been utilized to test the final design. These cadavers were provided by the Department of Anatomy, Faculty of Medicine and Surgery at the University of Malta. The operative dissection work was conducted at the Department of Anatomy. A comprehensive list of all equipment used during the clinical research is presented in Table 1.

Equipment	Model	Manufacturer	Country
5mm 30 degree endoscope	PE610A	Aesculap	Germany
3 chip Full HD camera system	PV460	Aesculap	Germany
LED light source	OP940	Aesculap	Germany
Maryland dissector	NA		
Laparoscopic scissors	NA		
Laparoscopic graspers	NA	Grena	UK
Prototype	NA	TU Delft	Netherlands

Table 1: List of equipment

3. Results

The results are divided into two sections: the final design and the results of the functional tests performed.

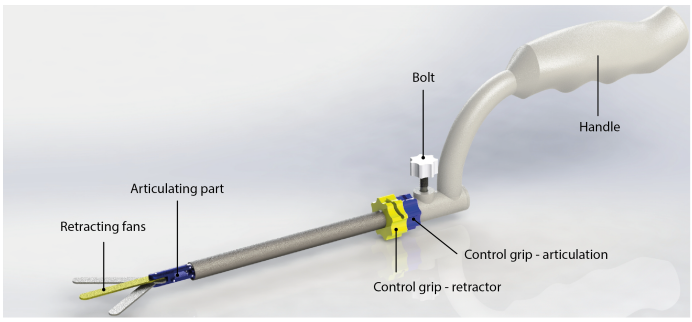

Figure 6: Final CAD design

Figure 7: Prototype with endoscope

3.1. Final CAD design

The final CAD design is a modular instrument with an outer diameter of 10mm, enabling the insertion of a standard 10mm trocar. The total length of the device is 395mm, including the handle, and 241mm without the handle. Most of the components are made of stainless steel, except for the control grips, the grip for the bolt, and the handle. These are made of resin with SLA printing, serving their purpose in the prototype phase. However, for production, injection molding with medical-grade plastic is preferred. Due to its modularity, there are no areas that cannot be accessed for cleaning or inspection. A final render is presented in Figure 6. The built prototype can be found in Figure 7. Most requirements are met in the digital model; requirements 9 to 13 were tested after the prototype was finished. The most important components are explained in the following sections.

3.1.1. User guide

The use of this device can be divided into five steps, as shown in Figure 8. The first two steps are executed before the procedure to make the process smoother and reduce setup time. In the first step, the inner system containing the articulation and fan controls is inserted into the outer tube until it reaches its limit, indicated by a notch on the holder rod that slides into the groove in the outer tube. In step two, the handle is slid over the outer tube until it reaches its limit, indicated by the control grips. At this point, the hole in the handle aligns

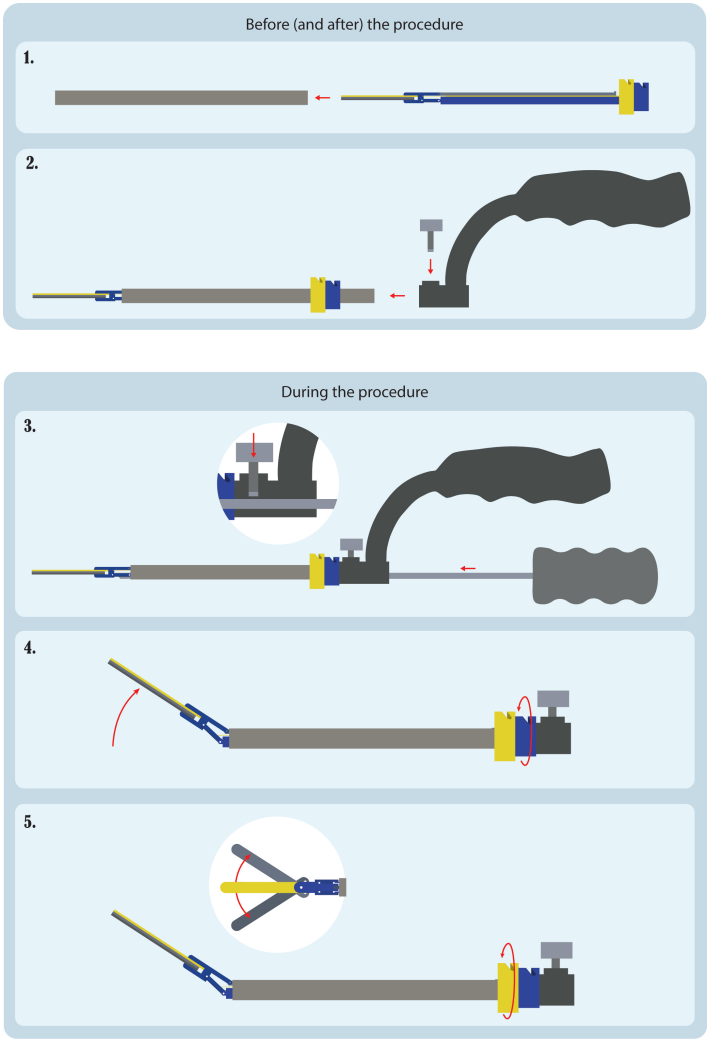

Figure 8: User steps

with a hole in the outer tube, allowing the bolt screw to be inserted to secure the handle and control mechanisms in place. The subsequent three steps are performed during the procedure. The endoscope is inserted into the device through the back of the handle. By tightening the bolt screw slightly further, the endoscope is clamped and securely held by the device (Step 3). This arrangement allows the assistant to hold only one handle, thus providing more space for the surgeon to perform the procedure. Once the device is inserted and positioned at the thyroid location, it can be articulated (Step 4) and retracted (Step 5) by manipulating the associated grips. Steps 4 and 5 can be executed independently of each other. After the tissue retrieval and completion of the procedure, all steps can be reversed to restore the device to its original state, remove it, and disassemble it for cleaning purposes.

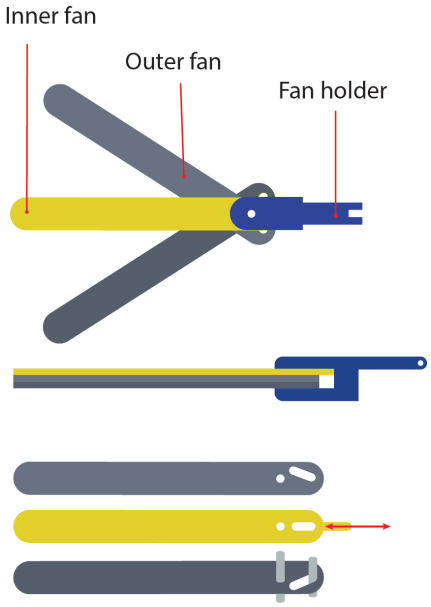

Figure 9: Fan detail

3.1.2. Fan Retractor

The retractor comprises three fans that expand when the central fan, highlighted in yellow in Figure 9, is retracted backward. The top fan connects to a spring leaf, which is, in turn, attached to the control rod. Each fan has grooves that allow a pin to slide through them. These grooves are oriented in different directions, causing two fans to extend outward when the central fan is pulled. The rod is secured by the fan holder, ensuring the pin remains stationary while only the fan moves relative to the pin. The outward movement is met with the most resistance due to the muscles and skin it displaces, while the inward motion will experience less resistance. Therefore, the grooves are designed to require pulling the fan for outward expansion, not pushing it. Another reason for this design choice is to minimize the risk of buckling of the spring leaf during pressing movements. The spring leaf is enclosed within the tip structure to reduce the potential for buckling further.

3.1.3. Articulation

The articulation is incorporated into the design to satisfy requirement 2, which aims to expand the workspace in the vertical direction. The principal components are depicted in Figure 10. By exerting forward pressure on the control rod, the h-profile applies force against the fan holder. The fan holder, constrained via the hinge provided by the holder rod, articulates in response to this force. Adopting the h-profile instead of conventional hinges is deliberate due to the h-profile's shape, which allows the endoscope to remain usable even when the articulation function is not engaged. While the view may be

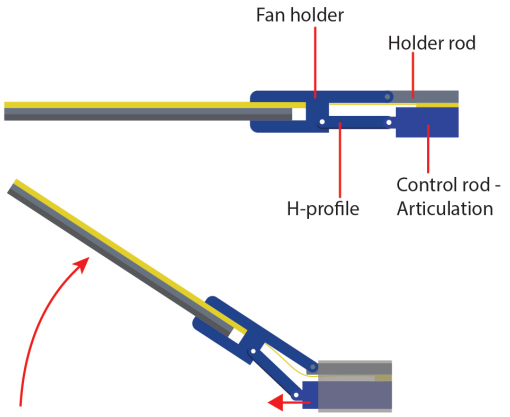

Figure 10: Articulation detail

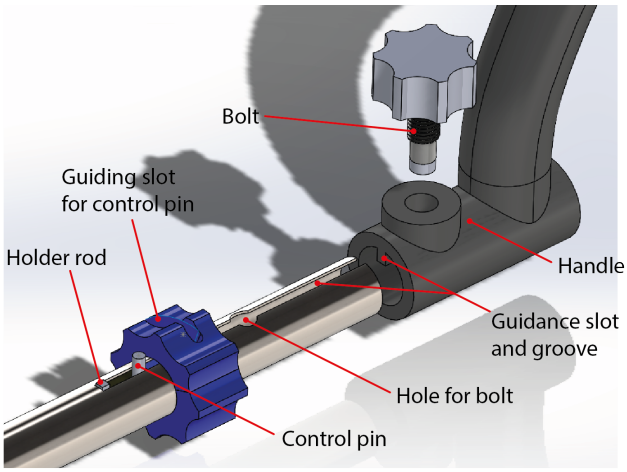

Figure 11: Back part detail

somewhat restricted within the h-profile, the endoscope remains operable, essential for device insertion. The closed top of the H-profile encases the spring leaf responsible for fan control, as mentioned in subsubsection 312. This additional feature is implemented as a precautionary measure to reduce the risk of buckling.

3.1.4. Control mechanism

The device is controlled using a cam-follower system; see Figure 11. By turning the control grip, a pin slides along the diagonal groove within this grip. The pin can only move along one axis, moving forward and backward when the grip is rotated. The system controlling the fans is colored yellow for visual purposes. The system controlling the articulation is colored blue. The fan is retracted using a stainless steel rod instead of a cable due to the rod's greater stiffness. The rod's stiffness provides enhanced control and the ability to withstand higher forces. The surgeon can exert both pulling and pushing actions, thereby regulating the outward and inward movements of the fans.

3.1.5. Modularity

The design is modular, such that it adheres to requirement 7. This is achieved by designing a system where the outer tube and inner elements can be detached. The control mechanism, including the control for the articulation and the fans, has a smaller overall diameter than the outer tube. This ensures that all the inner workings can slide out of the backside of the outer tube. When the device is in use, the inner system is closed in by the handle. The handle is secured by inserting the bolt through the handle and outer tube. By loosening or securing the bolt, the entire system can be removed or enclosed. Furthermore, the bolt can secure the endoscope by enclosing it internally, facilitated by its downward movement during bolt rotation.

3.2. Prototype

After the CAD model was transformed into a physical prototype, the design was assessed and its functionalities tested. The prototype was mostly made of stainless steel using wire electrical discharge machining. Only the top fan was made of spring steel because the spring leaf is made of the same material. Other elements not made out of stainless steel were the grips and handle, which were produced using stereolithography (SLA) 3D printing. The grips were made of two parts and were permanently assembled around the pins on the control rods using glue.

3.3. Study results

3.3.1. Functional requirements

The maximal retraction from the tip of the fans is measured to range from 43 to 39mm, depending on the articulation angle. The maximum articulation height is 31mm, and the angle is 24 degrees, as measured from the horizontal plane. The tip length measuring from the hinge point of articulation is 67.5mm, and the tips are 50mm long. The length of the insertable part is 187.5mm, including the tip.

3.3.2. Force tests

The preliminary force test to determine the necessary articulation force showed that a maximum force of 5.29N is needed to lift the skin enough for the surgeon to have enough vision. The mean force for all cadavers is 4.73N. The force measurements can be found in Table 2.

Inputting a total force of 5N into the SolidWorks simulation resulted in a maximum stress of 128.10 MPa in the articulated

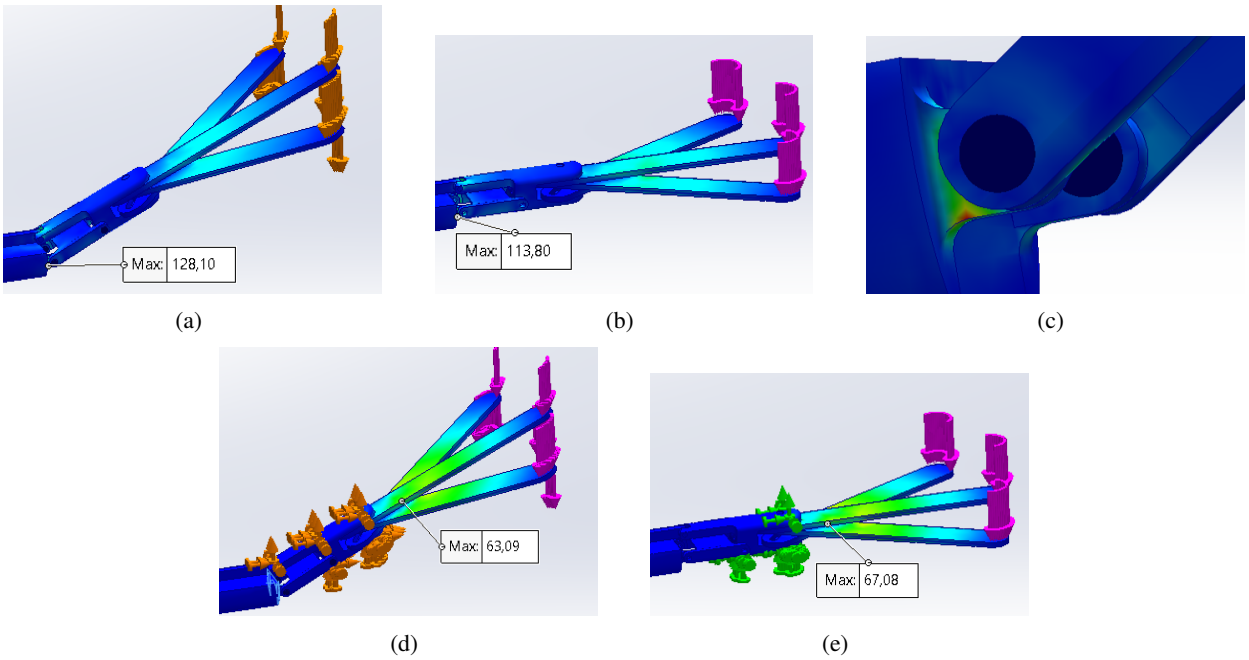

(a) (b) (c)

(d) (e)

Figure 12: (a) Stress with a force of 5N applied to the tip of the fans. The tip is on an angle, and the hinge is fixed; (b) Stress with a force of 5N is applied to the tip of the fans. The tip is horizontal, and the hinge is fixed; (c) The maximum stress point is located in the hinge that connects the control rod to the articulation and the h-profile. (d) Stress with a force of 5N applied to the tip of the fans. The tip is on an angle, and the fan holder is fixed; (e) Stress with a force of 5N is applied to the tip of the fans. The tip is horizontal, and the fan holder is fixed. The arrows show where the force is applied.

	Force (N)	**Preservation method**
Cadaver 1	3.97	Thiel embalmed
Cadaver 2	5.29	Thiel embalmed
Cadaver 3	4.61	Fresh frozen
Cadaver 4	5.05	Fresh frozen

Table 2: Forces measured in cadavers when lifting the skin.

position and a maximum stress of 113.80 MPa in the horizontal position. The maximum stress occurs at the hinge between the h-profile and the control rod for articulation, as shown in Figure 12c. When isolating the fan blades and applying the force to the tips, the maximum stress was 63.09 MPa in the articulated position and 67.08 MPa in the horizontal position. When 5N was applied to the prototype, the tip could articulate. In this case, the max articulation height reached 24mm at a 19-degree angle. Upon further inspection, the control pin for the articulation was broken. Furthermore, force measurements indicate that the articulation was backdrivable when a force of approximately 4N was applied to the fan tips.

3.3.3. Assembly test

Ten participants completed six iterations of both assembly and disassembly tasks, resulting in a total of 60 trials for each. All participants successfully executed the tasks without any issues, leading to the inclusion of all trials for analysis. Most trials exhibited a normal distribution, except for assembly trials 5 and disassembly trials 3, 4, and 5 (p=0.017, p=0.010, p=0.006, p=0.018, respectively). The first and last trials for both tasks displayed normal distributions. Using the paired samples t-tests, a significant difference was observed between the initial and final attempts of the assembly task (p=0.017), while no significant difference was found for the disassembly (p=0.063). Figure 13 illustrates boxplots of the performance results. The maximum assembly time recorded was 67.03s, with the shortest being 9.44s. For disassembly, the maximum time was 12.32s, and the shortest was 2.74s. On average, assembly tasks were completed in 20.21s, while disassembly tasks averaged 5.58s.

3.3.4. Pre-clinical test results

The surgeon was able to perform the procedure using the prototype. The device's dimensions were good, and the device was easy to handle and maneuver. Sufficient space was created in the cadavers to perform the procedure. However, due to its tight fit, it was not possible to move or remove the endoscope during the procedure. This made cleaning the lens difficult, as the entire prototype, including the endoscope, had to be

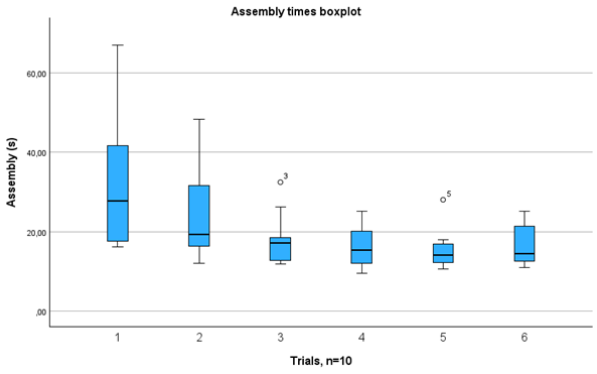

(a)

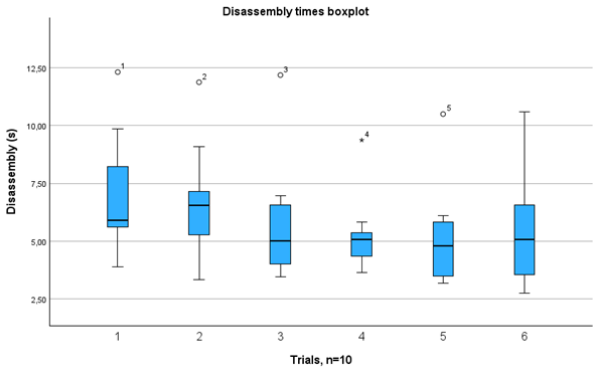

(b)

Figure 13: Boxplots per trial of the time for the task of assembly and disassembly.

	Removal time (s)
Cadaver 1	3.97
Cadaver 2	5.29
Cadaver 3	4.61
Cadaver 4	5.05

Table 3: The removal times measured in the pre-clinical study

removed each time for cleaning. The prototype could retract and articulate, although these functions were somewhat limited and could not reach the complete range that was possible outside of the body. In one case the tip bent further down than should have been possible, see Figure 16. The removal time was an average of 3.2s with a maximum time of 4.1s.

4. Discussion

4.1. Functional requirements

Most requirements were met. However, some prototype elements need improvement to adhere to the requirements. In Table 4, all of the requirements are briefly discussed. The first objective was fully met as a prototype design with space-maintaining capabilities suitable for use with a 5mm endoscope was achieved. The second objective mentions fully meeting all requirements, which have not yet been completely achieved. By making some adjustments to the design, these requirements and the objective will likely be met. The third objective compares and evaluates the prototype against the conventional CO_2 insufflation method. Although the surgeon did confirm that similar effects were achieved, a systemic comparison has not yet been made. The fourth and last objective was proven to be met during the pre-clinical test.

4.2. Prototype design

One notable observation during the measurement of the maximum retraction width was the difference between measurements in the non-articulated and articulated states (43mm vs 39mm). This discrepancy is likely attributed to the tension exerted on the spring leaf when transitioning into the articulated state. As the tip's angle changes, there is a slight increase in length. However, achieving the maximum retraction in the articulated state is possible if the tip is first retracted and then articulated. This is most likely the order in which the prototype would be used, so this should not pose a problem.

4.3. Cleanability

The design's modularity ensures reusability by facilitating cleaning. While currently, all parts are accessible, certain areas may pose greater difficulty in reaching them. Adhering to some general guidelines outlined by Horeman *et al.* [27], it is recommended that all areas be easily accessible for brushing and cleaning, with all parts visible for visual inspection to ensure proper cleaning. The round grips, attached in the prototype using glue, present a challenge as they cannot be removed for cleaning, resulting in difficult-to-clean areas within these grips and preventing complete separation of inner parts. However, a spreader can be used during washing to spread the control rod of the articulation and the fan apart, see Figure 15. To improve accessibility, the grips could be designed to be removable for cleaning. One potential approach is to incorporate a hinge point, allowing them to be easily clamped around the pins.

4.4. Testing

4.4.1. Force testing

The force test to determine the retraction force was conducted utilizing two Thiel-embalmed cadavers and two fresh-frozen cadavers, resulting in a mean force of 4.73N. However, the

Functional requirements	Requirement fulfillment
1. The device should maintain a workspace for the surgeon to have a clear visualization of the thyroid anatomy, which translates to a maximum width of 50mm and a minimum length of 50mm of the tip in the expanded state of the device.	This requirement is met, with an articulating length of 67.5mm and a fan length of 50mm. This is the result of design choices that were made.
2. The device should create a space above the thyroid with a minimum height of 30mm to allow for adequate freedom of movement for the endoscopic tools. This is to accommodate the (steerable) tips, which have a length of approximately 30mm when pointed downwards.	This requirement is met. However, the maximum height decreased after extensive testing, and the prototype was not able to reach full articulation in the cadavers, which did not meet the requirement in the necessary context.
3. The outer diameter in its smallest state should be no more than 10mm. This is to accommodate insertion through a 10mm trocar cannula which is used in a standard TOETVA procedure.	This requirement is met. The outer diameter is 10mm and fits through a trocar.
4. The device must have a space for a 5mm endoscope to be inserted and used during surgery.	This requirement is met since the endoscope fits into the prototype. However, the fit was too tight for it to be removed easily. Thus, the design would need minor adjustments in margins for the endoscope to be able to move through the space with ease.
5. The insertable part of the device must have a minimal length of 150mm to be able to reach the surgical site and to accommodate the 100mm length of the trocar.	This requirement is met, as the insertable part of the prototype is 187.5mm. However, this length does not offer support for a standard 300mm long endoscope, which is fragile. Furthermore, due to its length, the grips interfere with the nose. Making the tube longer could eliminate these problems.
6. The tip of the instrument should be able to articulate with a force of 10N without undergoing deformation. This is double the force needed to lift the skin.	This requirement is not met. It could articulate when applying a force of 5N, but the pin came loose. For a force of 4N, the control grip for articulation becomes backdriveable. Furthermore, a deformation is observed in the fans. Material changes and changes in the design of the grips and tip could offer different results.
7. All regions of the device must be able to be reached by the appropriate standard cleaning brushes for cleaning, which in the case of closed regions means the device must be modular and able to be disassembled to be able to reach these areas.	This requirement is partly met. The inner components of the prototype can be removed from the outer tube, which gives access to otherwise difficult-to-reach areas. However, some parts are still difficult to reach. These areas stay contained within the grips, as these are not modular in the prototype.
8. The instrument must be able to be sterilized using common sterilization methods (autoclave).	This requirement is not met. As some parts of the prototype are made using PLA 3D printing, this material is unsuitable for the autoclave. Changing this material into RVS would mitigate this problem.
9. The device should not obstruct the endoscope's field of view when the retractor is fully articulated.	This requirement is party met. When the prototype is articulated, and the endoscope is inserted, the prototype is entirely out of view. But as the prototype was unable to articulate in the cadaver, this requirement is only met if the articulation issue is dealt with.
10. It should be possible to execute the procedure with two endoscopic instruments without collision with the camera system.	This requirement is met. The surgeon can perform the procedure without any collision.
11. A single person can assemble the device in less than 110 seconds.	This requirement is met, with a maximum assembly time of 67.03 s and an average of 20.21 s.
12. A single person can disassemble the device in less than 110 seconds.	This requirement is met, with a maximum disassembly time of 9.44 s and a mean time of 5.85 s.
13. In case of bleeding, the device should be removable within three steps and within 12 seconds to free up the neck area for a traditional open thyroid surgery.	This requirement is met. The maximum time to remove the device was 3.2s, below the required time. Three steps are needed to remove it: reverse retraction, reverse articulation, and pull out of the trocar.

Table 4: Functional requirements with a brief discussion on their fulfillment

measurements solely captured the vertical force necessary to displace the skin, neglecting potential shear forces generated during the retractor's movement within the body. Nevertheless, these forces are comparable to those reported in existing literature. Notably, no prior studies were found investigating the forces required to displace both the skin and platysmal muscle in the neck. However, research on displacing colon tissue revealed a force requirement of 4.7N [29]. Similarly, another source reported a force of 4.59N exerted by a transvaginal endoscope in a pig [30]. Despite the differences in tissue type, structure, and thickness, these values align closely with the measured force, affirming its suitability for device testing purposes.

When a force of 5N is applied in the Solidworks simulation, the maximum stress point reached was 128.10 Mpa. This value is below the yield strength of the material, which was 275 Mpa in the simulation. It should be noted that the maximum stress point occurs specifically in one of the hinge points rather than in the fans, as depicted in Figure 12c. Increasing the fillets and reducing the number of sharp corners is recommended to alleviate the stress at this point. It is advised that further research and design optimization be done to achieve the most favorable stress distribution. When clamping the fan holder, the maximum stress is 67.12 Mpa for a force of 5N with the tip in

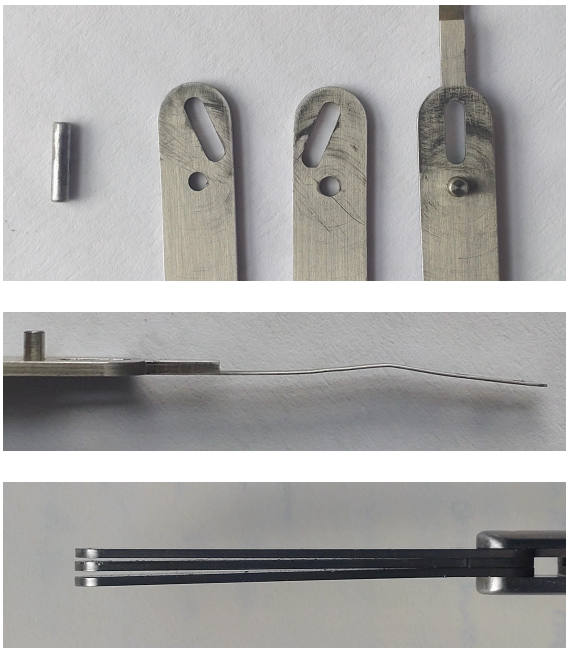

Figure 14: Damage observed in various components of the prototype after testing. (a) Both the pin and grooves show signs of wear; (b) The spring leaf also shows signs of permanent deformation caused by the buckling; (c) Plastic deformation observed in the fans

the horizontal position, which is well below the yield strength. According to this simulation, the stresses within the prototype should not exceed its yield strength and, thus, not have any plastic deformation. However, upon inspection of the prototype after the procedures, some plastic deformation can be detected in the fans; see Figure 14. There could be several reasons for the discrepancy between the results obtained from a simulation and the actual reality. One possible explanation could be that the simulation does not accurately predict the model. This could be due to the nonlinearity of the material or large deformations. To obtain more realistic results, performing a non-linear analysis in a more suitable program is suggested. Another possibility is that the force measured in the cadavers is not correct. The force test only measured the force required to pull up the horizontal area of the fans and did not consider the fact that the area stretched is much larger since the tube of the tool occupies space from the mandible to the tip. However, some of this area is also caused by the trocar, which takes up some forces. Additionally, when testing the simulation with double the force (10N), the fans still did not plastically deform, which suggests that the problem lies with the simulation. A third option is that the prototype's material properties are not similar to those in the simulation.

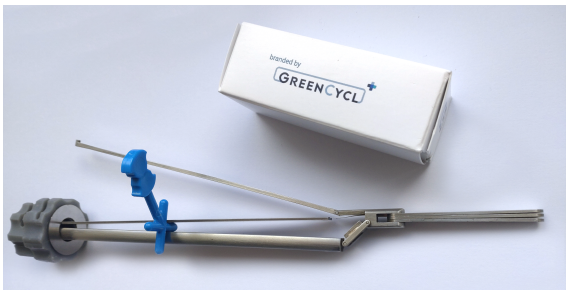

Figure 15: A demonstration of how the spreader from GreenCycle could be used to access the difficult-to-reach areas during cleaning.

This deformation could be limited by replacing the fans with medically graded hard steel.

When a force of 5N is applied to the prototype, it can articulate. However, the angle and maximum height were considerably lower than when the prototype was measured without the added force. Upon inspection of the device, it was observed that the pin had become loose. This resulted in the tip being able to move without turning the grip. This could indicate that the forces on the pin are too high or may be due to improper assembly. Investigating the forces acting on the pin and modifying the design is recommended. Furthermore, the tip exhibited backdrivability around 4N, which should be avoided in future designs. To decrease the likelihood of backdrivability, the friction between the pin and slot should be reduced. One approach could involve changing the material of the grips to increase friction between the pin and slot. Alternatively, adjusting the angle of the slot in the grip is another option. However, this may necessitate increasing the length of the groove to maintain the same relative distance, potentially complicating manufacturing the grips from two parts.

4.4.2. Assembly experiment

The average assembly and disassembly times are 20.21s and 5.85s. These are both below the set requirement of 110s. This was the longest measured disassembly time amongst the largest Dutch academic medical centers [27]. Statistical analysis comparing the initial and final trials revealed a significant difference in assembly times, suggesting the presence of a learning curve. However, no significant difference was detected for disassembly. Nonetheless, this is not concerning given that the average and maximum disassembly times recorded were well within the required time (5.85s, 12.32s). During the testing of the prototype, the fans encountered an increasing amount of friction each time it was handled until they were completely unable to retract. Upon disassembling the tip fans, several observations were made. Firstly, noticeable wear was observed on the slots and pin where they made contact, with the slots

exhibiting minor indentations. The damage to these components is depicted in Figure 14. Secondly, there was a distinct change in the thickness of the fans next to the slots compared to their thickness at the opposite end. This deformation is presumed to result from the force exerted by the pin on the slots, causing material deformation and outward shifting. Consequently, this localized increase in thickness, approximately 0.02mm per fan, totaling 0.04mm for the two fans, heightened friction to a point where sliding became impossible. To limit this problem, the following changes could be made. Firstly, the material that is used now is stainless steel. Changing this material into hardened steel could limit the amount of wear the parts would encounter. Secondly, introducing a slight curvature to the fans could enhance control over the clamping force. The problem occurred mainly after extensive repetitive testing of the assembly. During the removal of the inner system from the outer tube, the fans occasionally extend outwards due to their relative positioning to other components. If these distances change during removal, the fans are forced outwards against the outer tube, leading to an application of force onto the slots. To address this, design alterations could be implemented to ensure that during removal, the grips remain attached to the holder rod, thereby preventing the outward sliding of the fans. While a fully functional prototype was developed, achieving optimal materials and production methods proved challenging. Differences in material could potentially impact the stiffness of the tips. Moreover, certain design choices were made due to the limited availability of machinery, which may have been altered if alternative manufacturing options were available. An example of this is the length of the prototype. Because the length is below 150mm (for the inner system), these parts can all be made using wire electrical discharge machining. However, the limitation of this method is that it has a maximum length of material that can be processed.

4.4.3. Pre-clinical testing

The preclinical study was performed to assess the prototype's functional requirements in cadavers. The first observation was the endoscope's tight fit in the prototype. Increasing the margin in the hole through which the endoscope passes could resolve this issue. The most noticeable problem was the inability to articulate when inserted into the cadavers. The force transmitted through the grips proved insufficient to displace the prototype adequately for skin elevation. The grip also had to be held continuously because the control system was backdrivable with a force bigger than 4N. Furthermore, there were instances where the articulation mechanism bent downward, exceeding its intended range and risking damage to the prototype, depicted in Figure 16. In the fourth cadaver, the pin connecting to the middle rod controlling the articulation had become loose again. This could have been a reason why the tip was bending downward. As this is the second time it has come loose, this suggests that the forces on the pin might be higher than expected. This should be inspected in further research. Another factor contributing to the bending downward was the increasing space between the grips observed as the procedure progressed. Given that the linear displacement of the controlling pins is only 2mm, an additional space of 1mm effectively halved the articulation distance. Enhancing the effectiveness of the articulation could involve modifying the material and shape of the grips. However, it is also essential to assess the tip to ensure the hinges can withstand the force exerted on them. The fans of the prototype did have difficulty retracting when inside the body. It is possible that the forces to displace the skin were too high to retract properly. However, it was observed that the fans could retract in less constrained spaces, indicating that proper skin dissection might enhance retractability. Similar to the articulation, the force transmission from the grips was not enough, so this should have been improved. Notably, the difference in camera view with or without retraction was minimal. Nonetheless, if the endoscope could articulate freely, it could offer a larger workspace below the fans. The position of the grips scratched the nose, affecting usability and causing potential damage. Replacing these grips with top-mounted pins could alleviate this issue and provide better grip control for the assistant, also limiting the problem of insufficient force transmission. Although the surgeon deemed the prototype's length sufficient, the protrusion of the endoscope out the backside by approximately 10 cm posed a risk of damage due to its fragility. Lengthening the prototype would limit this risk and allow the grips to position more towards the back, reducing collisions with the nose. Examination of the prototype after the procedure revealed that the pin attached to the control rod for the fans had become loose, and the fans themselves were slightly bent, likely due to excessive forces. Changing the shape of the fans, giving them a slight curvature, could limit this deflection.

4.5. Recommendations

Some future research should be done on the redesign of the fans to avoid plastic deformation and the issue with the pin and grooves. Also, the design of the grips should be reconsidered to offer a bigger force transmission and limit the space between the grips. Due to the limited articulation function in the pre-clinical cadaver study, we could not produce sufficient images of the phases of the procedure which could then be compared to the same phases of the procedure using CO_2 gas insufflation. By comparing the visual feedback among surgeons, comparing surgical times, and checking post-operative damage to the cadavers, the new design should be compared to the more conventional TOETVA with CO_2 insufflation. This should all be considered for future research.

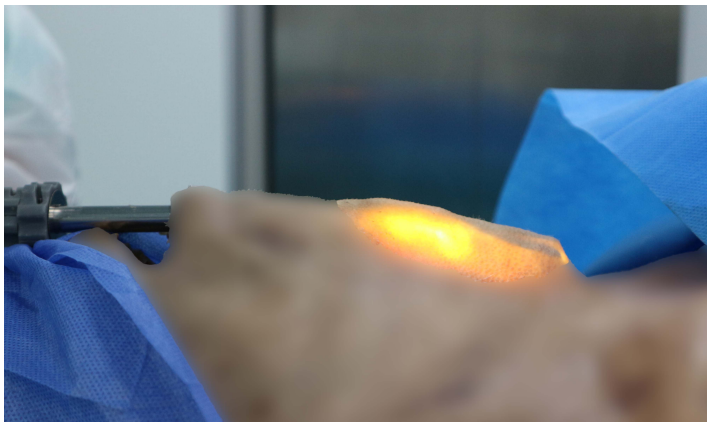

Figure 16: Side view of the prototype when inserted into the body. The tip is bent downwards

4.6. Relevance of procedure

There is an ongoing debate regarding the relevance of TOETVA compared to conventional open surgery, given that its primary advantage lies in cosmetic outcomes [31][32][33]. Numerous studies have compared TOETVA to conventional open surgery (OT), with open surgery demonstrating superior results in terms of operational time, post-surgical inflammation, and cost [31]. However, no significant difference has been found in major complications between OT and TOETVA (2.1% vs. 1.5%) [34]. Additionally, some improvement in post-operative pain has been observed [16]. Thus, besides the main benefit of positive cosmetic results, TOETVA offers other advantages. Nevertheless, the cosmetic benefits should not be underestimated. Some studies have found that although participants expressed anxiety and self-consciousness about the scar during the earlier healing stages (2-6 weeks), this concern diminished over time, with satisfaction and quality of life returning to pre-operative levels after 2 years [35][36]. However, these studies did not account for potential cultural and gender biases in post-surgical aesthetics due to limited diversity within participant groups. Furthermore, the median age of participants being middle-aged adults may not adequately reflect the varying importance of aesthetics across different life stages. A study examining scar perception up to 5 years post-surgery revealed a particularly noticeable negative effect among Asian and Afro-Caribbean individuals, underscoring the importance of cultural considerations [37]. African American patients demonstrated lower scar perception satisfaction compared to white patients [38]. Some patients may prefer the cosmetic benefits of TOETVA over the surgical benefits of open surgery. Seventy-five percent of participants expressed a preference for an extra cervical scar, especially females under 60 years old, even if it entails additional costs, increased travel times, and a higher risk of recurrent laryngeal nerve (RLN) and mental nerve damage [39]. Overall, the literature suggests that a considerable number of patients experience a decline in postoperative quality of life (QoL), with endoscopic approaches potentially enhancing both body image and self-perception [32][4]. However, patient selection is crucial when considering performing TOETVA. Selection criteria may be based on patient preference, tumor size, and disease nature. Advanced cancer or a large goiter size may necessitate OT [16]. Thus, while patient selection is vital to maximize safety and outcomes, TOETVA remains a safe and effective procedure, particularly for individuals with specific cultural backgrounds. Overcoming higher costs and increased procedure time could offer significant benefits to these individuals.

5. Conclusion

This study aimed to develop a device that could maintain a spacious workspace during the Transoral Endoscopic Thyroidectomy Vestibular Approach (TOETVA) without using co_2 gas. We have designed a new gasless modular retractor tailored for compatibility with a standard endoscopic camera. This project has successfully achieved three of the objectives. Despite not fully meeting all of the requirements, the incorporation of our newly designed instrument into surgical procedures shows promise. However, further research is necessary to improve the articulation force of the design and compare its performance with conventional CO2-based TOETVA methods. Such comparative studies are crucial for validating the effectiveness of our design against established methods and determining its full potential and efficacy in clinical practice.
[1]

[1] All of the images in this paper are created by the author.

REFERENCES

[1] Sosa J. A. Kitahara, C. M. The changing incidence of thyroid cancer. *Nature Reviews Endocrinology*, 12(11):646–653, 2016.

[2] National Cancer Institute. Seer cancer stat facts: Thyroid cancer. `https://seer.cancer.gov/statfacts/html/thyro.html`, Accessed at January 11, 2024.

[3] C. Chen, S. Huang, A. Huang, Y. Jia, W. Ji, M. Mao, J. Zhou, and L. Wang. Total endoscopic thyroidectomy versus conventional open thyroidectomy in thyroid cancer: a systematic review and meta-analysis. *Therapeutics and Clinical Risk Management*, 14:2349–2361, 2018.

[4] Y. Choi, J. H. Lee, Y. H. Kim, Y. S. Lee, H. S. Chang, C. S. Park, and M. R. Roh. Impact of postthyroidectomy scar on the quality of life of thyroid cancer patients. *Annals of Dermatology*, 26(6):693, 2014.

[5] Y. Ikeda, H. Takami, M. Niimi, S. Kan, Y. Sasaki, and J. Takayama. Endoscopic thyroidectomy and parathyroidectomy by the axillary approach. *Surgical Endoscopy And Other Interventional Techniques*, 16(1):92–95, November 2001.

[6] T. D. Duncan, I. A. Ejeh, F. Speights, Rashid Q. N., and M. Ideis. Endoscopic transaxillary near total thyroidectomy. *JSLS*, 10(2):206–211, 2006.

[7] Titus D. Duncan, Qammar Rashid, Fredne Speights, and Ijeoma Ejeh. Transaxillary endoscopic thyroidectomy: An alternative to traditional open thyroidectomy. *Journal of the National Medical Association*, 101(8):783–787, August 2009.

[8] Y. Ikeda, H. Takami, G. Tajima, Y. Sasaki, J. Takayama, H. Kurihara, and M. Niimi. Section 2. thyroid. *Biomedicine amp; Pharmacotherapy*, 56:72–78, November 2002.

[9] Ohgami M, Ishii S, Arisawa Y, Ohmori T, Noga K, Furukawa T, and Kitajima M. Scarless endoscopic thyroidectomy: breast approach for better cosmesis. *Surg Laparosc Endosc Percutan Tech*, 10(1):1–4, 2000.

[10] Eui Suk Sung, Yong Bae Ji, Chang Myeon Song, Bo Ram Yun, Won Sang Chung, and Kyung Tae. Robotic thyroidectomy: Comparison of a postauricular facelift approach with a gasless unilateral axillary approach. *Otolaryngology–Head and Neck Surgery*, 154(6):997–1004, March 2016.

[11] Kyung Tae, Yong Bae Ji, Chang Myeon Song, and Junsun Ryu. Robotic and endoscopic thyroid surgery: Evolution and advances. *Clinical and Experimental Otorhinolaryngology*, 12(1):1–11, February 2019.

[12] K. Witzel, B. H. A. von Rahden, C. Kaminski, and H. J. Stein. Transoral access for endoscopic thyroid resection. *Surgical Endoscopy*, 22(8):1871–1875, December 2007.

[13] Thomas Wilhelm and Andreas Metzig. Endoscopic minimally invasive thyroidectomy (emit): A prospective proof-of-concept study in humans. *World Journal of Surgery*, 35(3):543–551, November 2010.

[14] Cunchuan Wang, Hening Zhai, Weijun Liu, Jinyi Li, Jingge Yang, Youzhu Hu, Jing Huang, Wah Yang, Yunlong Pan, and Hui Ding. Thyroidectomy: A novel endoscopic oral vestibular approach. *Surgery*, 155(1):33–38, January 2014.

[15] Angkoon Anuwong. Transoral endoscopic thyroidectomy vestibular approach: A series of the first 60 human cases. *World Journal of Surgery*, 40(3):491–497, November 2015.

[16] Angkoon Anuwong, Khwannara Ketwong, Pornpeera Jitpratoom, Thanyawat Sasanakietkul, and Quan-Yang Duh. Safety and outcomes of the transoral endoscopic thyroidectomy vestibular approach. *JAMA Surgery*, 153(1):21, January 2018.

[17] Kyu Nam Kim, Dong Won Lee, Ji Yeon Kim, Kyoung-Hee Han, and Kyung Tae. Carbon dioxide embolism during transoral robotic thyroidectomy: A case report. *Head amp; Neck*, 40(3), December 2017.

[18] Jinbo Fu, Yezhe Luo, Qinggui Chen, Fusheng Lin, Xiaoquan Hong, Penghao Kuang, Wei Yan, Guoyang Wu, and Yiyao Zhang. Transoral endoscopic thyroidectomy: Review of 81 cases in a single institute. *Journal of Laparoendoscopic amp; Advanced Surgical Techniques*, 28(3):286–291, March 2018.

[19] Eun Young Park, Ja-Young Kwon, and Ki Jun Kim. Carbon dioxide embolism during laparoscopic surgery. *Yonsei Medical Journal*, 53(3):459, 2012.

[20] Jinxi Jiang, Gaofei He, Junjie Chu, Jianbo Li, Xiaoxiao Lu, Xianfeng Jiang, Lei Xie, Li Gao, and Deguang Zhang. Gasless submental-transoral combined approach endoscopic thyroidectomy: a new surgical technique. *Frontiers in Oncology*, 13, May 2023.

[21] Jun-Ook Park, Yeong Jun Park, Mi Ra Kim, Dong-Il Sun, Min-Sik Kim, and Yoon Woo Koh. Gasless transoral endoscopic thyroidectomy vestibular approach (gasless toetva). *Surgical Endoscopy*, 33(9):3034–3039, May 2019.

[22] Jinxi Jiang, Gaofei He, Junjie Chu, Jianbo Li, Xiaoxiao Lu, and Deguang Zhang. Novel suspension system for gasless transoral vestibular thyroidectomy. *Surgical Endoscopy*, 37(2):1070–1076, September 2022.

[23] Jun-Ook Park, Soo-Geun Wang, Dahee Park, In-Ho Bae, Jin-Choon Lee, Byung-Joo Lee, and Sung-Chan Shin. The feasibility of a prototype thyroidoscope for gasless transoral endoscopic thyroidectomy: A preclinical cadaver study. *Journal of Laparoendoscopic amp; Advanced Surgical Techniques*, 29(7):953–957, July 2019.

[24] C. Camenzuli, J. Attard, J. C. Borg, P. Schembri-

Wismayer, J. C. Borg, and J. Calleja-Agius. Cadaveric evaluation of a device supporting gasless transoral endoscopic thyroidectomy. *Surgical Innovation*, 27(4):410–411, 2020.

[25] Salvatore Benvenga, Giovanni Tuccari, Antonio Ieni, and Roberto Vita. *Thyroid Gland: Anatomy and Physiology*, page 382–390. Elsevier, 2018.

[26] G. Dionigi, A. Bacuzzi, M. Lavazza, D. Inversini, V. Pappalardo, L. Boni, S. Rausei, M. Barczyński, R. P. Tufano, H. Y. Kim, and A. Anuwong. Transoral endoscopic thyroidectomy via vestibular approach: operative steps and video. *Gland surgery*, 5(6):625–627, 2016.

[27] T. Horeman, F. Schilder, M. Aguirre, G. M. M. J. Kerkhoffs, and G. J. M. Tuijthof. Design and preliminary evaluation of a stiff steerable cutter for arthroscopic procedures. *Journal of Medical Devices*, 9(4), August 2015.

[28] A.G.C. van Boeijen, J.J. Daalhuizen, J.J.M. Zijlstra, and R.S.A. van der Schoor. *Delft Design Guide*. BIS publishers, Amsterdam, 4 edition, 2013.

[29] H. Visser, E.A.M. Heijnsdijk, J.L. Herder, and P.V. Pistecky. Forces and displacements in colon surgery. *Surgical Endoscopy*, 16(10):14263–1430, October 2002.

[30] Priya a. Jamidar, Charles a. Mosse, Margherita Cadeddu, Michael Boyd, and Paul Swain. Retraction force measurement during transgastric and transvaginal notes. *Gastrointestinal Endoscopy*, 67(5):AB119, April 2008.

[31] Mehmet Taner Ünlü, Nurcihan Aygun, Erdinc Serin, and Mehmet Uludag. Comparison of transoral endoscopic thyroidectomy vestibular approach and open conventional thyroidectomy regardıng inflammatory responses, pain, and patient satisfaction: a prospective study. *Frontiers in Surgery*, 10, November 2023.

[32] Samantha A. Wolfe, Victoria E. Banuchi, and Jonathon O. Russell. Quality of life after remote access thyroid surgery: a narrative review. *Annals of Thyroid*, 7:9–9, August 2022.

[33] Moon Young Oh, Young Jun Chai, Hyeong Won Yu, Su-Jin Kim, June Young Choi, and Kyu Eun Lee. Transoral endoscopic thyroidectomy vestibular approach as a safe and feasible alternative to open thyroidectomy: a systematic review and meta-analysis. *International Journal of Surgery*, 109(8):2467–2477, May 2023.

[34] Jonathon O. Russell, Zeyad T. Sahli, Mohammad Shaear, Christopher Razavi, Khalid Ali, and Ralph P. Tufano. Transoral thyroid and parathyroid surgery via the vestibular approach—a 2020 update. *Gland Surgery*, 9(2):409–416, April 2020.

[35] Kathy Bach, Samantha Prince, Susan C. Pitt, Sarah Robbins, Nadine P. Connor, Cameron Macdonald, Rebecca S. Sippel, and Kristin L. Long. Time heals most wounds — perceptions of thyroidectomy scars in patients with thyroid cancer. *Journal of Surgical Research*, 270:437–443, February 2022.

[36] Sasha K. Kurumety, Irene B. Helenowski, Sneha Goswami, Benjamin J. Peipert, Susan E. Yount, and Cord Sturgeon. Post-thyroidectomy neck appearance and impact on quality of life in thyroid cancer survivors. *Surgery*, 165(6):1217–1221, June 2019.

[37] Asit Arora, Chloe Swords, George Garas, Konstantinos Chaidas, Alexa Prichard, James Budge, D. Ceri Davies, and Neil Tolley. The perception of scar cosmesis following thyroid and parathyroid surgery: A prospective cohort study. *International Journal of Surgery*, 25:38–43, January 2016.

[38] Stuti P. Garg, Abbas M. Hassan, Anooj Patel, Deima Koko, Jeffrey Varghese, Marco F. Ellis, John Y.S. Kim, and Robert D. Galiano. Scar perception: A comparison of african american and white self-identified patients. *Plastic and Reconstructive Surgery - Global Open*, 10(5):e4345, May 2022.

[39] Rupporn Sukpanich, Santi Sanglestsawai, Carolyn D. Seib, Jessica E. Gosnell, Wen T. Shen, Sanziana A. Roman, Julie A. Sosa, Quan-Yang Duh, and Insoo Suh. The influence of cosmetic concerns on patient preferences for approaches to thyroid lobectomy: A discrete choice experiment. *Thyroid*, 30(9):1306–1313, September 2020.

APPENDIX A
ANATOMICAL STRUCTURES

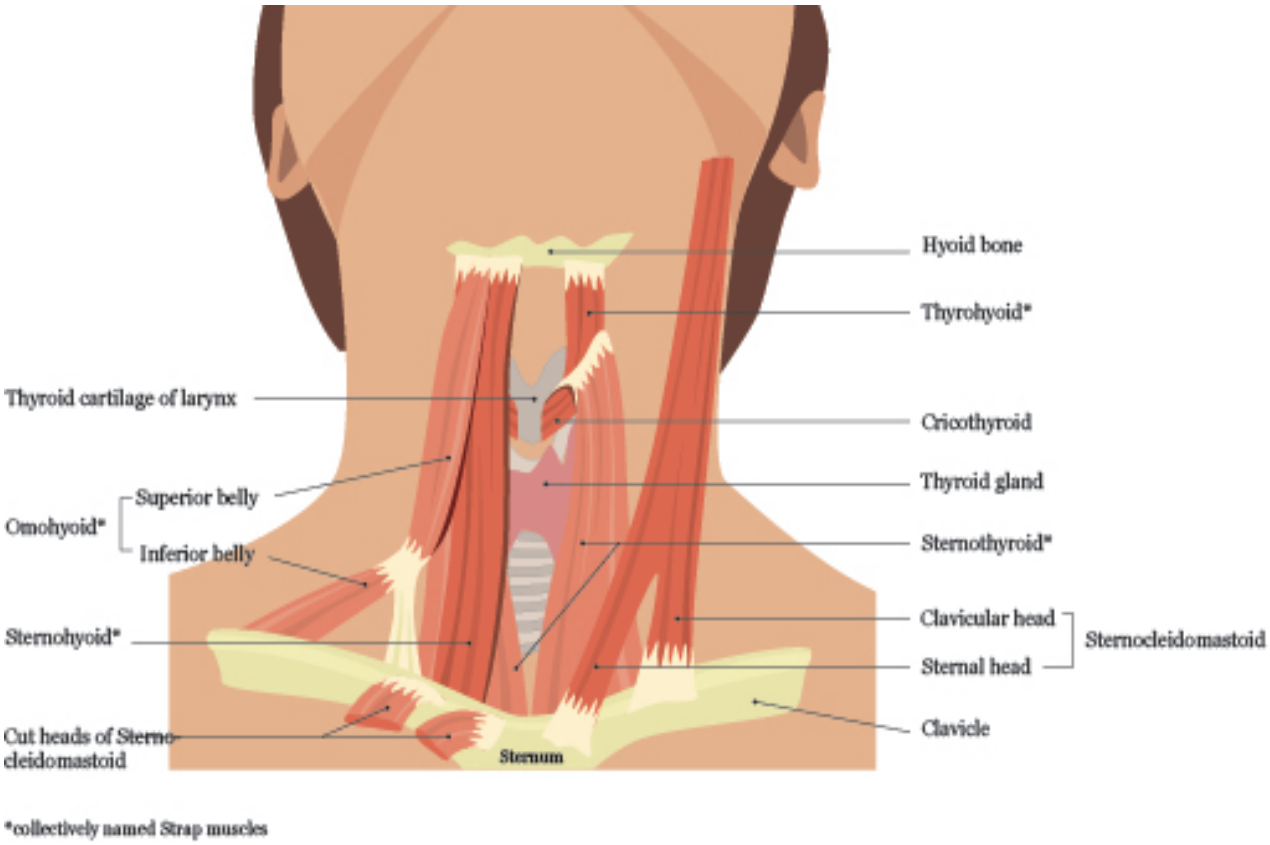

Figure 17: Anatomy front view

APPENDIX B
DESIGN PROCESS

B1. Mindmap for each different sub-functions

For all of the sub-functions, a mindmap was made, except for ”Insertion”. The content for the mindmaps was found using patent and literature searches.

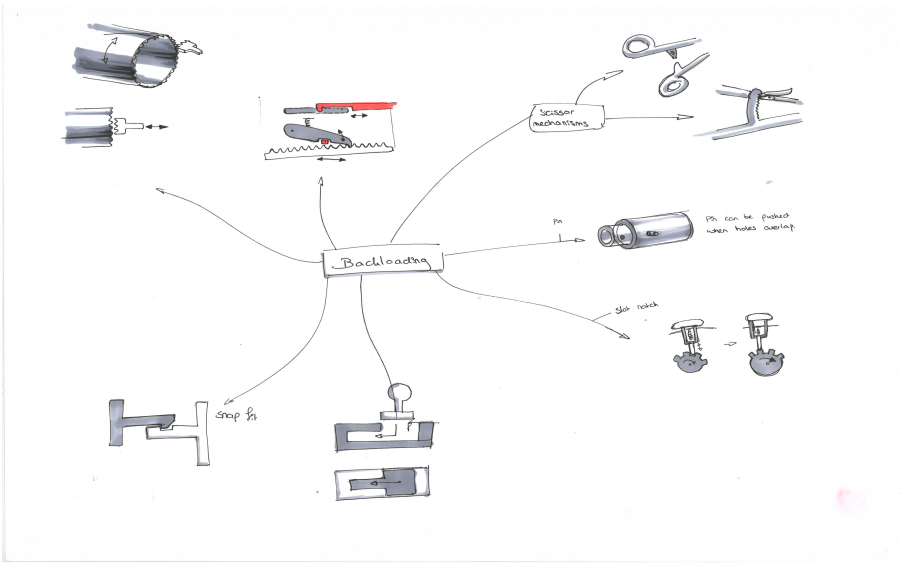

Figure 18: Mindmap - backloading

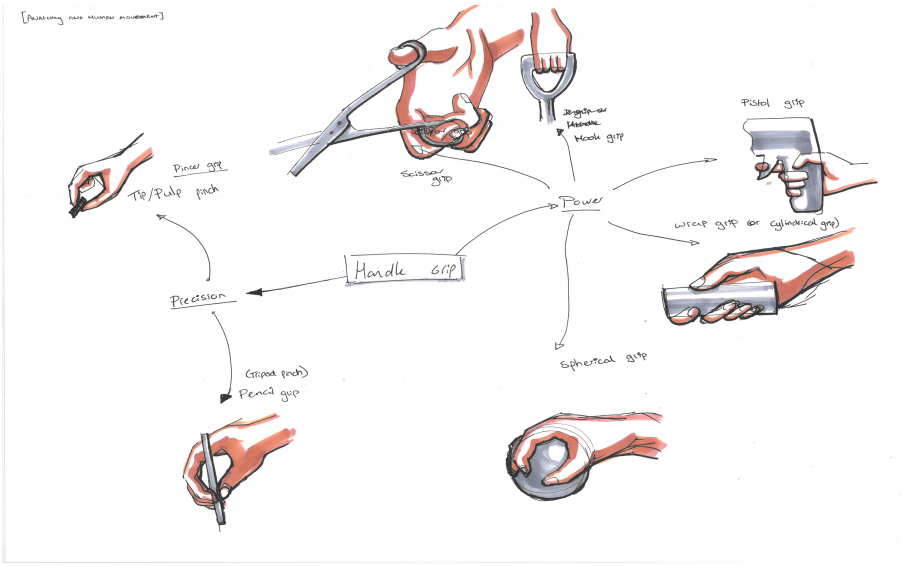

Figure 19: Mindmap - Handle grip

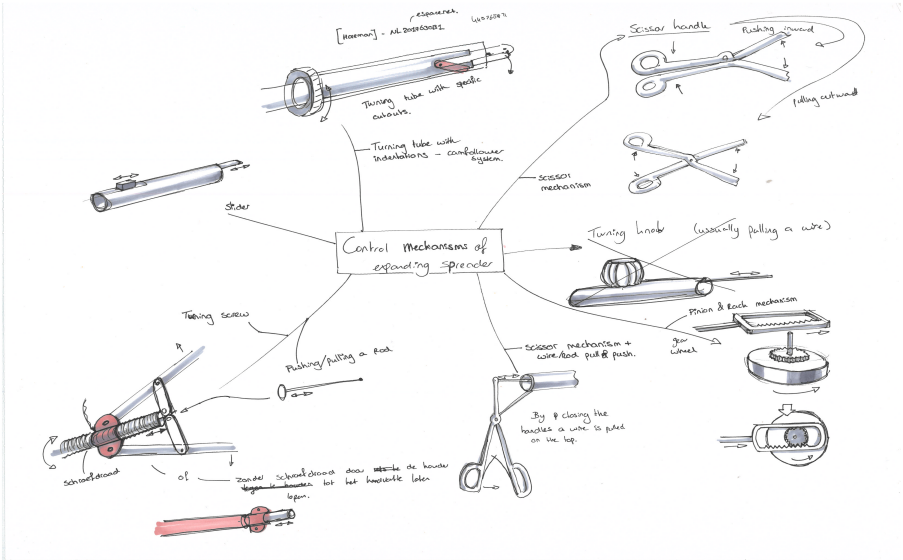

Figure 20: Mindmap - Control mechanisms

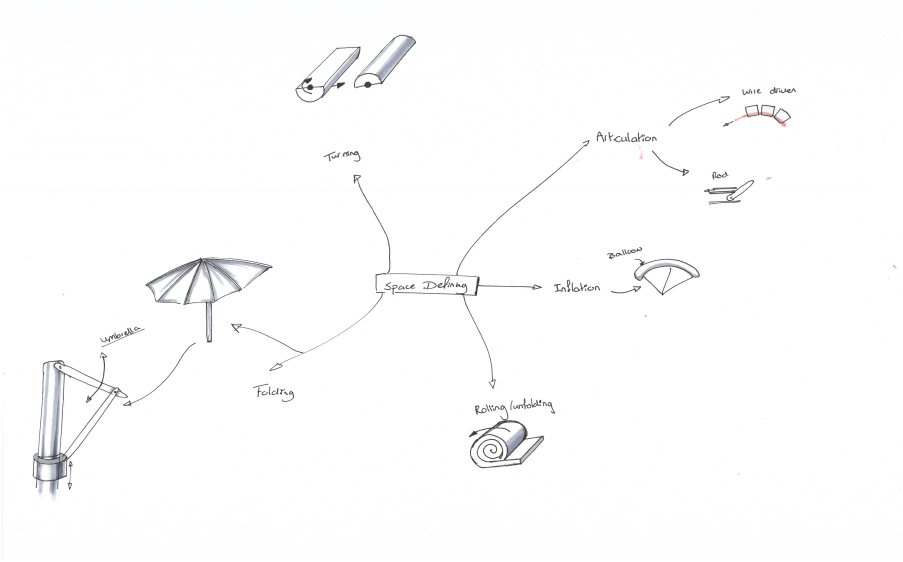

Figure 21: Mindmap - space definition

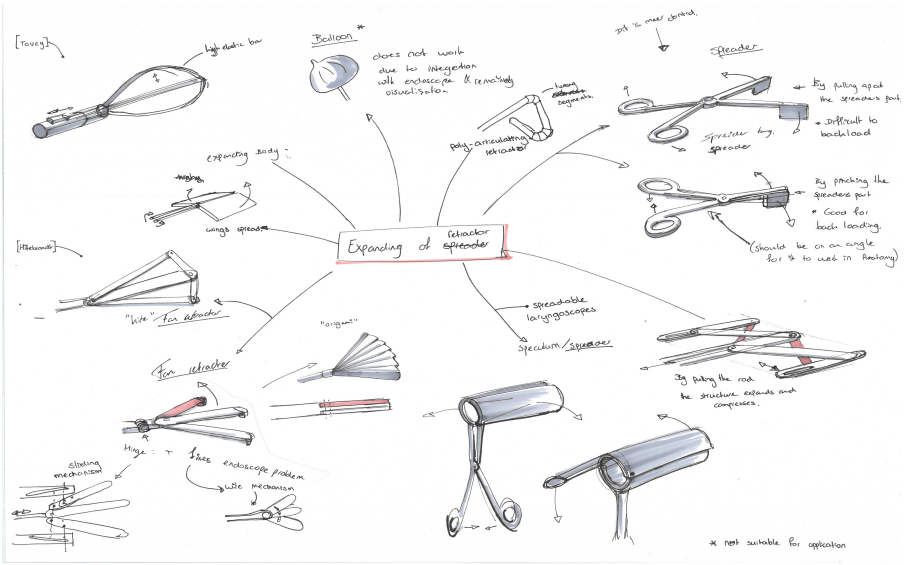

Figure 22: Mindmap - Expanding of retractor

B2. Morfological map

The morphological map was formed with all of the sub-functions (y-axis) and partial solutions (x-axis), as can be seen in Figure 23.

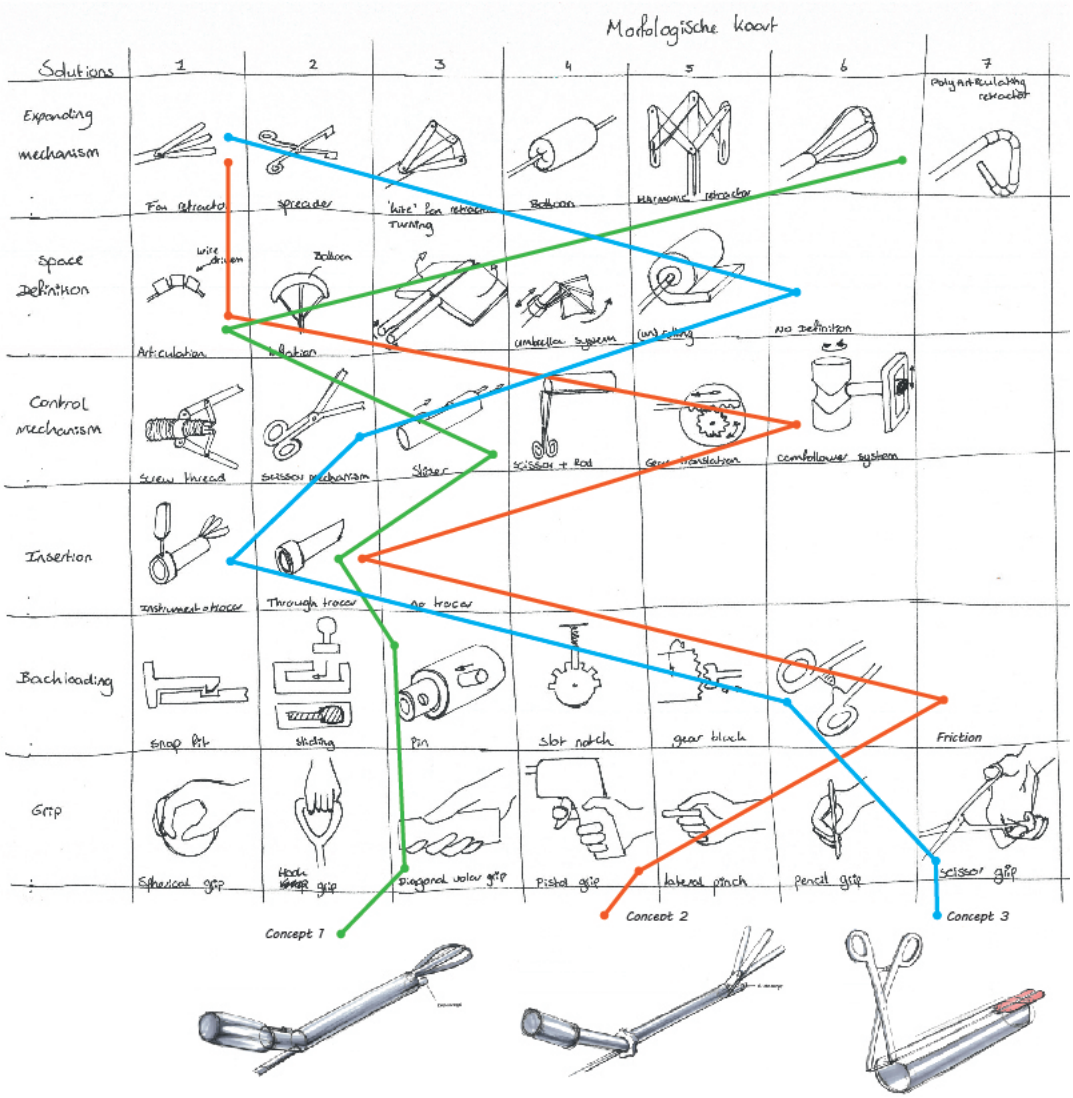

Figure 23: Morfological map

B3. Concept drawings

Concept 1 was a combination of flexible metal rods, with a sliding mechanism and a pin lock. The downside of this design is that the flexible rods might not offer enough force than needed to displace the skin. Concept 2 has a combination of a fan retractor with articulation and a cam-follower control mechanism. It is similar to concept 1 in the articulation and design. They are also both meant to fit through the trocar. In concept 3 the trocar and retractor are combined into one device. It does not have an articulating element, since the retractor is already at the top of the trocar and therefore higher in the operating space than in the other two designs. Concept 2 was chosen to develop further into a final design. This design has a fan retractor at the tip which can articulate by a rotational movement at the proximal end.

B4. Harris Profile

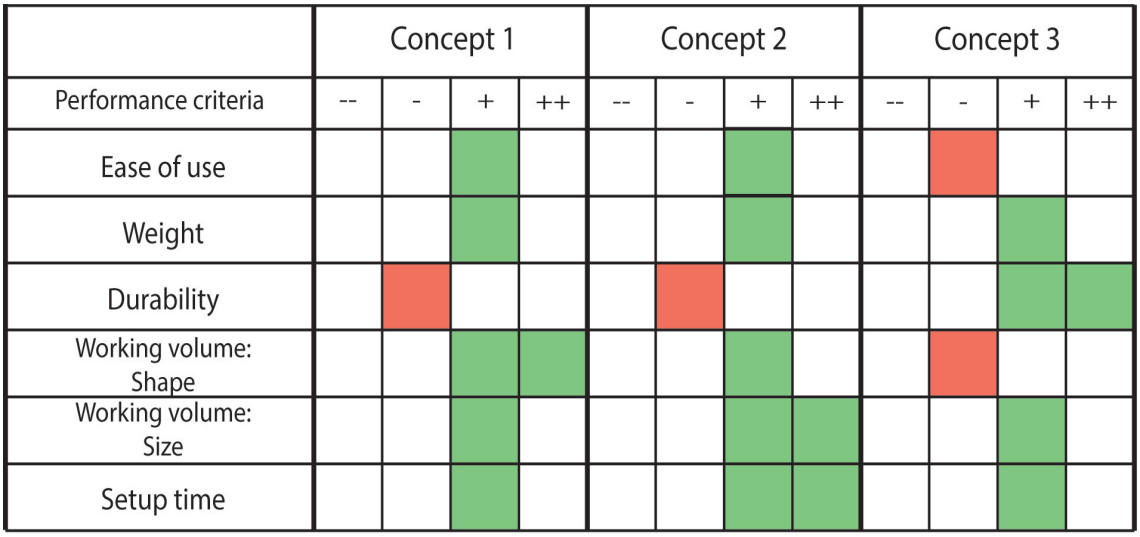

Figure 24: Harris profile

B5. Design iteration

The device has undergone multiple iteration cycles. The first design was created to develop a functional prototype and test the concept. This version included the articulation and fan system but did not have control for both systems. However, it proved the working principle of the two systems combined and the control of one of the systems. The next iteration aimed to perfect the device for standard operation. While designing this version, the assembly steps were taken into account. The primary focus was to create a prototype that could meet all the requirements. The most significant change in this version was that the fan holder was attached to the holder rod instead of the outer tube. This allowed the entire system to be removed from the outer tube for cleaning, making the device compliant with requirement 7. Another change was the profile of the middle tube, which was redesigned based on the surgeon's feedback to make efficient use of the limited space. Once the design seemed acceptable, the next iteration focused on assembly and manufacturability. Experts in these fields collaborated to make changes that would make production easier. This resulted in a change in the control grips, where the grip was assembled around the pin to make it easier to slide over the pin. Another difference in the final design was the shape of the fan control rod, which was made rectangular to simplify manufacturing. The bolt in the handle was also added in this version, which helped to clamp the endoscope to the device, as requested by the surgeon. A nylon cap was put on the end of the bolt to reduce the point pressure on the endoscope when clamping, as it is a delicate instrument.

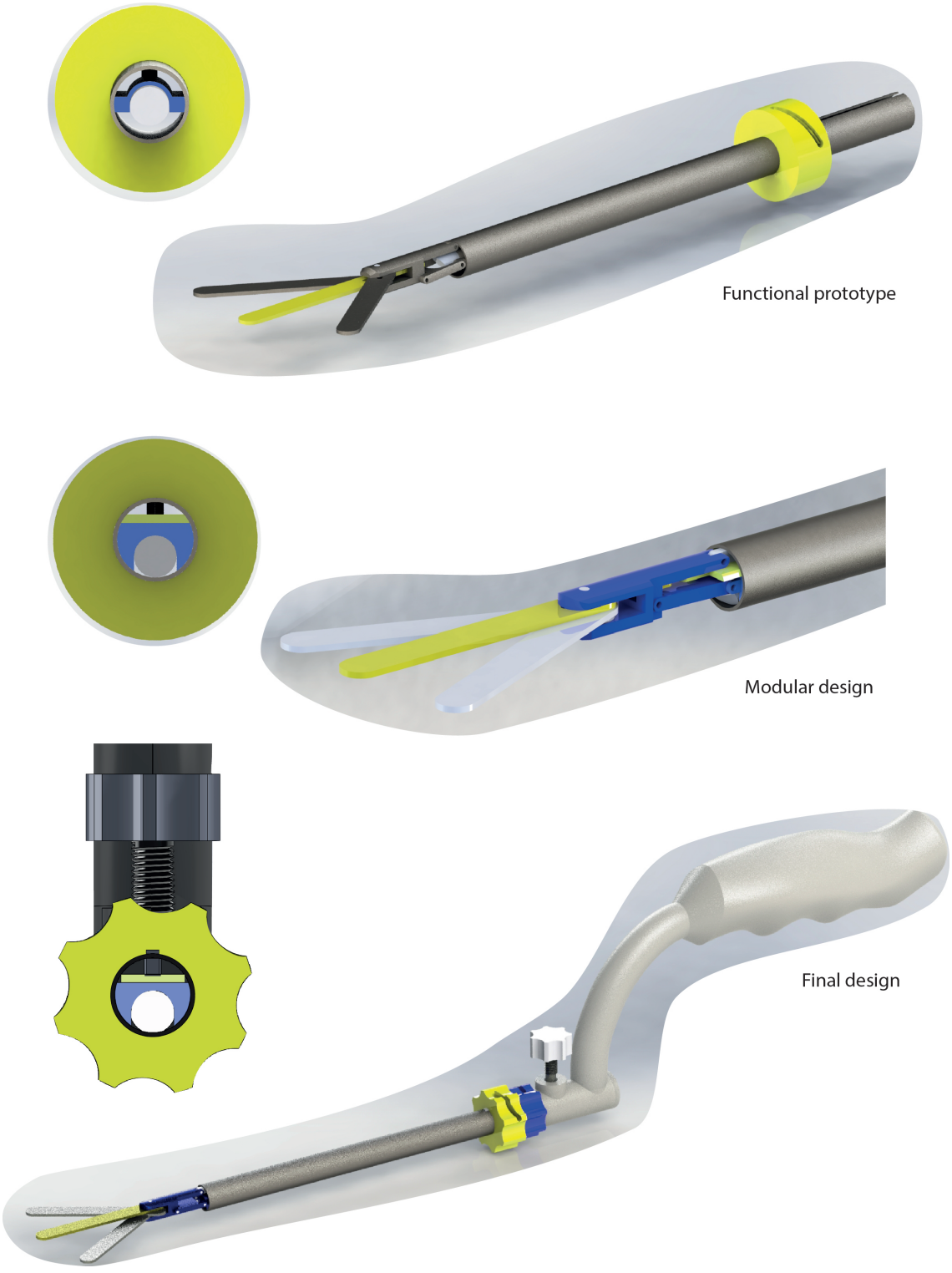

Figure 25: Design iterations